DESIGN OF AN ARRAY OF GERMANIUM DETECTORS FOR EXPERIMENTS WITH FAST RADIOACTIVE BEAMS

T. Glasmacher, P.G. Hansen, V. Maddalena, P. Mantica, D.J. Morrissey, M. Thoennessen, and A. Wagner

A number of experiments performed at the NSCL over the past two years attest to the important role that the detection of gamma rays can play in nuclear structure studies with radioactive beams at intermediate energies. However, they also very clearly demonstrate the limitations imposed by the use of scintillation detectors with very modest energy resolution. Early in 1997 we submitted a proposal to the NSF Major Research Instrumentation Program for the acquisition of a high-efficiency segmented germanium array to be used in nuclear structure experiments at the NSCL. In September 1997 this proposal received funding from the NSF with a cost-sharing complement from MSU. We have carried out a design study to find the most cost-effective solution and to ensure that the assumed performance is realistic. The results of this design study, which was completed in February of 1998, are reported here.

1. Measurements of Gamma rays Emitted from a Moving Source: Lorentz Boost and Doppler Shift

We note initially that our planned application differs in an essential way from that of high-spin physics, which for a long time has been the leading source of innovation in experiments with large germanium arrays. For these experiments it has been quintessential to be able to extract minute branches from extremely complex spectra having very high gamma multiplicities. Technically this is done by setting multiple gates on gamma rays that are shared by the particular branch of interest. Consequently, there is a high premium on resolving power and thus on high *absolute* photopeak detection efficiency (see e.g. [1]). In our applications, we expect events with low multiplicity and can only hope to see those excitations that exhaust a substantial fraction of the cross section for the total reaction channel. We shall demonstrate in the following that this leads to a situation where resolution can be traded against count rate and vice versa. The optimal solution is then the one that gives the highest count rate for a given minimum energy resolution required[+].

The NSCL Coupled Cyclotron Project, foreseen to be completed in the year 2001, will increase the intensities of the radioactive beams by typically a factor 10^3 and deliver secondary beams with energies around 100 MeV/u. In the following examples we have taken this as our reference energy and discuss first some of the major factors that affect the design.

The Lorentz boost of the intensity in the forward direction is illustrated in Fig. 1, which clearly shows how important this is for the detection efficiency of an array of limited size. For a source with isotropic emission in the CM system the gain is a factor of 2.5 in the forward direction and a factor of 0.4 in the backward direction. There is clearly a premium on placing the detectors close to 0°. The necessarily low intensity of radioactive beams makes this less inconvenient than it would be in experiments with stable beams. In Fig. 2 we show the total intensity per element of angle for neutrons and charged fragments arising from collisions of a mass 34 projectile with a light target. Outside a cone of 10°-12° the particle dose will be low.

In order to investigate the basic design options we considered a model in which a fixed area of germanium is placed symmetrically around the beam axis. Rather arbitrarily we assumed 370 cm^2 of detector packed with a surface coverage of 50%. In most radioactive-beam experiments the beam intensity is not a

[+] A perspicuous referee commented on or proposal that it is unfortunate that no viable detector system has yet been developed to fill the niche between the ultrahigh resolution of hyperpure solid-state detectors such as germanium and scintillation detectors such as sodium iodide and BGO. We agree.

free parameter, rather, one works with the maximum available. This leaves only two free parameters, the target thickness and the target-to-detector distance. In order to construct a figure of merit for this situation we assume that one gamma ray taken to have an energy of 1 MeV is produced per mg/cm^2 of target and we calculate the peak response for a given experimental arrangement. This calculation was performed summing the response in all detectors and calculating the overall resolution with all contributions to the standard deviation (including the intrinsic resolution) summed in quadrature.

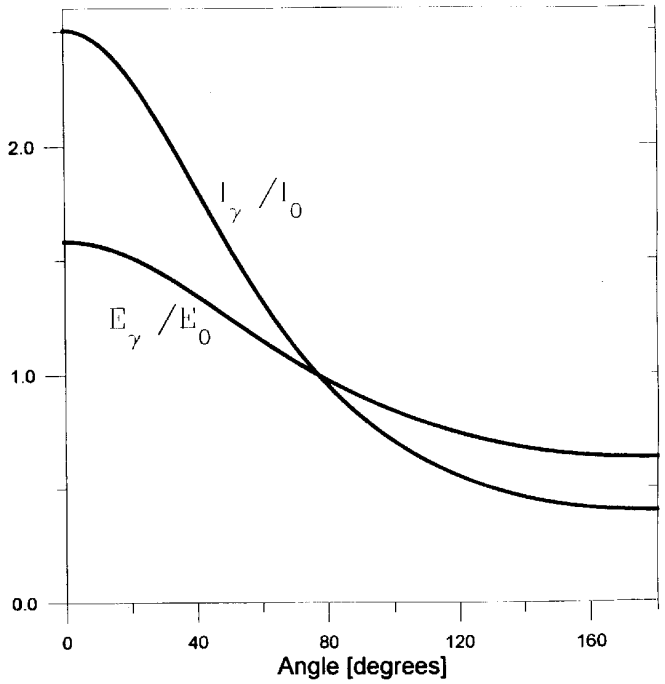

Figure 1: Effect of the Lorentz boost for a 100 MeV/u projectile on the gamma-ray energy and intensity as a function of the laboratory angle relative to the beam axis.

For two different detector arrangements, the results obtained in this calculation are shown in Figs. 4 and 5. The figures suggest that for a given experimental situation a choice must be made between count rate and resolution. The performance at the "magic" angle of 64.5[a] turns out to be comparable to that at the forward angles.

2. Design Considerations

The discussion in section 1 has tacitly assumed that we know the point from where a gamma ray was emitted. Fig. 6 demonstrates that this point can safely be assumed to be the immediate vicinity of the target for the vast majority of E1, E2 and M1 electromagnetic transitions. We note in this connection that E2 transitions normally are considerably faster while E1 transitions are very much slower than the Weisskopf estimate. Isomers living longer than some tens of nanoseconds will decay in the beam stop and can be studied at rest there.

It is also necessary to know the momentum vector of the fragment emitting the gamma ray. Since in the majority of all experiments with radioactive beams, the reaction product suffers little deflection relative

---

For clarity we outline how the measures of dispersion were handled in these estimates. A rectangular response of width W translates into a standard deviation of $\sigma = 12^{-1/2}W$. Conversion between standard deviation and resolution is taken to be FWHM = 2.35σ, valid for a Gaussian line shape. The line shapes regenerated after Doppler correction deviate strongly from Gaussians on the wings of the lines.

to the beam direction, typically a few degrees or even less, this correction can easily be made given that we must in any case identify the mass, charge and momentum of the fragment.

To lowest order then, all that we need is the angle of the gamma ray relative to the beam axis. This suggests the arrangement shown in Fig. 7. The detector is a single crystal, with the outer contacts segmented into eight 1cm wide discs. The gamma rays enter perpendicularly to the symmetry axis of the crystal and in a plane containing the beam axis. Considerations that we shall outline below suggest that there is no sharply defined optimum for the granularity, but that 1cm lateral segments provide a cost-efficient solution. The further subdivision of the discs into quadrants provides approximately a 3 cm granularity (again in terms of a rectangular response) in the less important left/right and forward/backward dimensions. We estimate that this is sufficient to account for the non-axial emission of the reaction fragment.

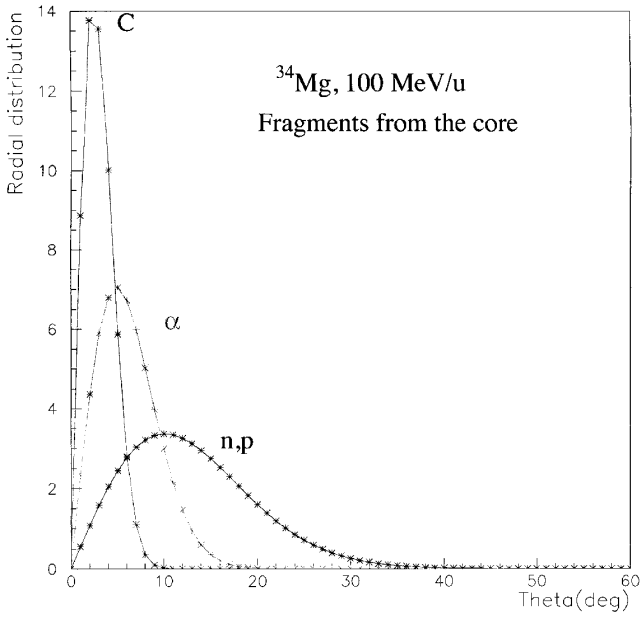

Figure 2: Estimated intensity per unit angular interval for core fragments produced in breakup of a mass 34 projectile. The curves are normalized to the same area.

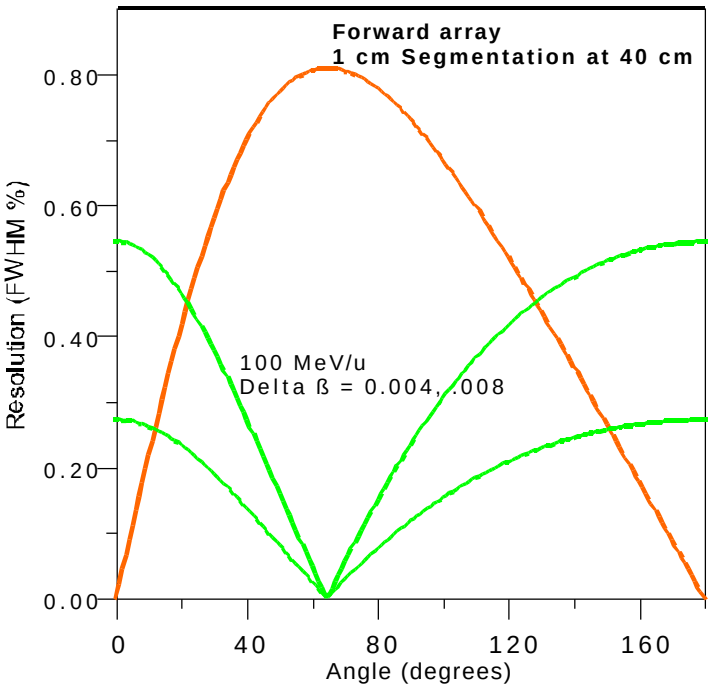

Figure 3: Contribution to the resolution (in % of the gamma energy) from (i) the slowing down of the projectile from front to back of the target corresponding to 0.004 and 0.008 in units of v/c (These examples correspond to 100 MeV/u manganese and tin ions, respectively, traversing a 50 mg/cm^2 gold target.), and from (ii) a granularity of the detector of 1cm expressed as the rectangular response function seen at a distance of 40 cm.

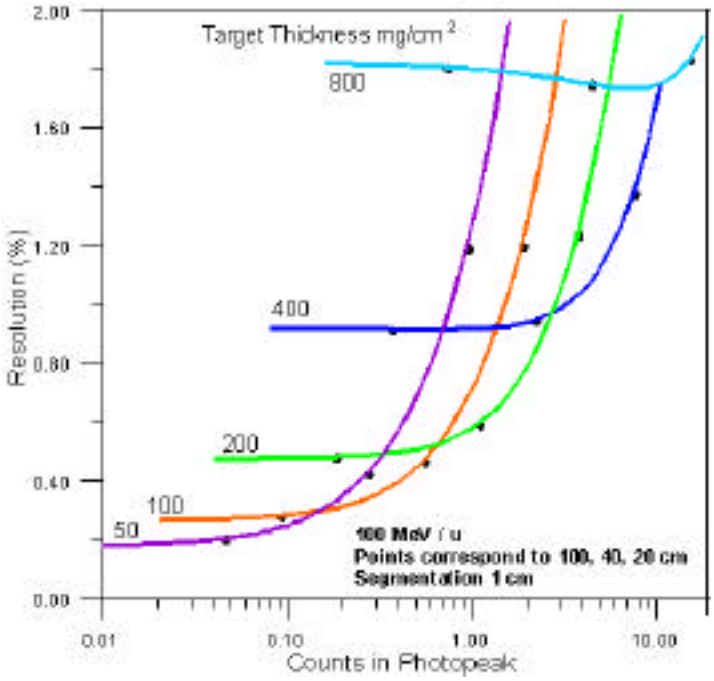

Figure 4: Performance of the forward array with basic parameters discussed in the text. The resolution is expressed as the full width at half maximum (FWHM). The points for each target thickness mark the target-to-detector distances 100, 40, and 20 cm.

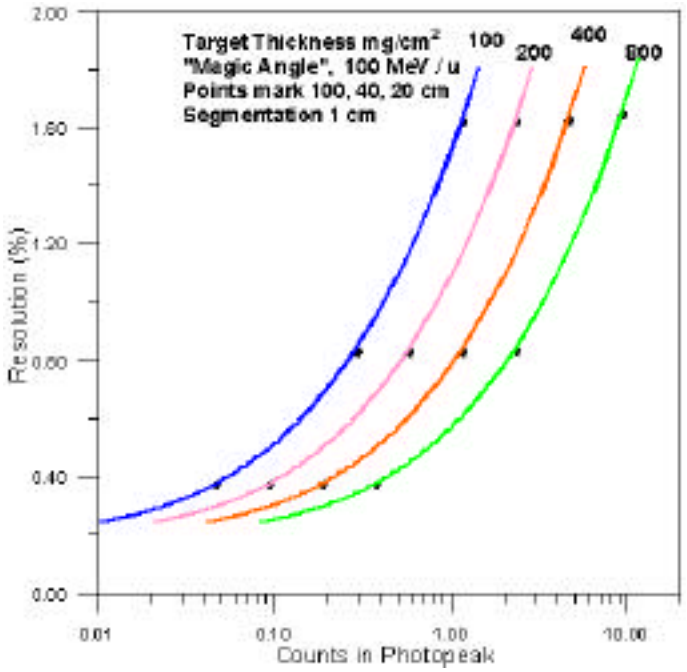

Figure 5: Same as Fig. 4 but with the array centered around the "magic" angle of 64^0, see Fig. 3.

Current research on segmented germanium detectors (see e.g. [2]) shows that pulse-shape information will allow an interpolation of the position coordinates within a given segment and hence give greatly improved spatial resolution. It will be possible to implement these techniques in our proposed array at a later stage when the necessary electronics modules are commercially available. The arrangement in Fig. 6 as well as its associated electronics, which we will not discuss here, based entirely on existing technology and should allow us an early start on the physics program.

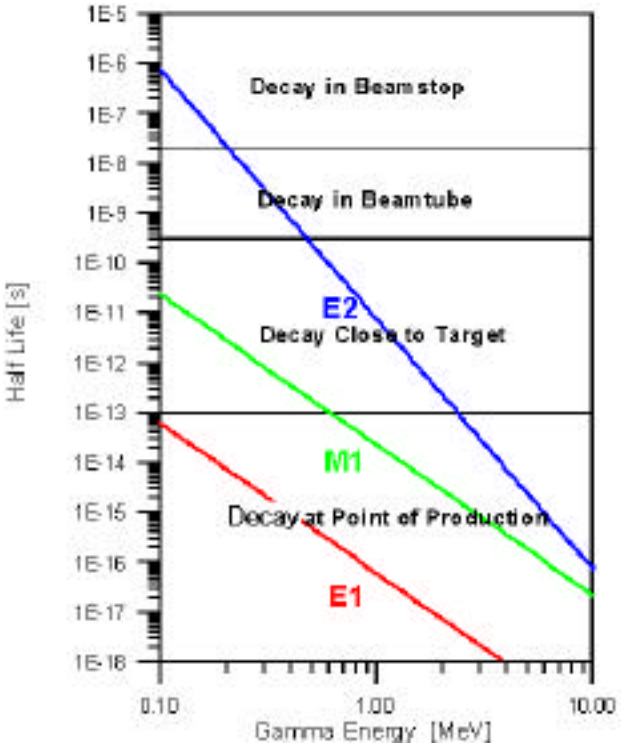

Figure 6: The Weisskopf estimates of the half lives in seconds for E1, E2 and M1 electromagnetic transitions for a nuclear fragment of mass 40 compared with the scales of experimental interest. Th transition probabilities were calculated from the expressions given in [4] and are not strongly dependent on mass. The effect of internal conversion, which makes the half lives appreciably shorter for heavy nuclei and low gamma energies have not been included.

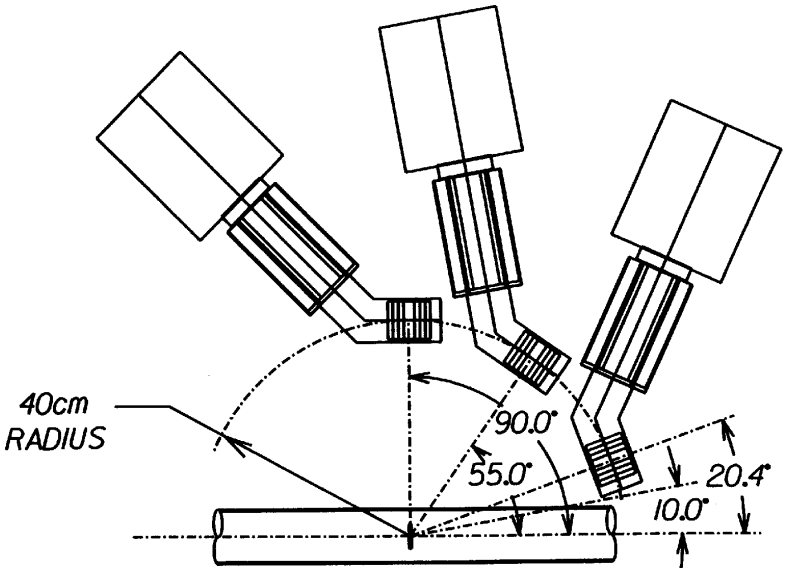

Figure 7: Proposed arrangement of the germanium detectors relative to the beam axis. More detectors can be placed at different azimuthal angles around the beam axis. The detectors in the illustration are 7 cm diameter germanium cylinders, 8 cm long and with the external contacts subdivided to give 8 discs, each 1 cm long. The gamma rays enter perpendicular to the detector's cylinder axis. The energy signal is obtained from the hollow axial contact, while the external contacts provide position information. Each disc is further subdivided into four quadrants (not shown) so that the total localization identifies a given signal with a granularity of 1 cm (axial direction) times approximately 3 cm in the lateral and depth directions.

Given the conceptual design solution of Fig. 7, we now ask the following questions:

(i) Is the efficiency for lateral impact of the gamma rays comparable to that of the more traditional axial impact?

(ii) If several cells are active in an event, how do we select the one that corresponds to the point of impact?

(iii) Given the answer to (ii), what is the resulting energy resolution and line shape when an observed event is retrocorrected to the rest system of the recoiling nucleus?

(iv) What is gained by increasing the number of segments? Is there an optimum?

These questions have been investigated in a series of Monte Carlo simulations, which we now discuss.

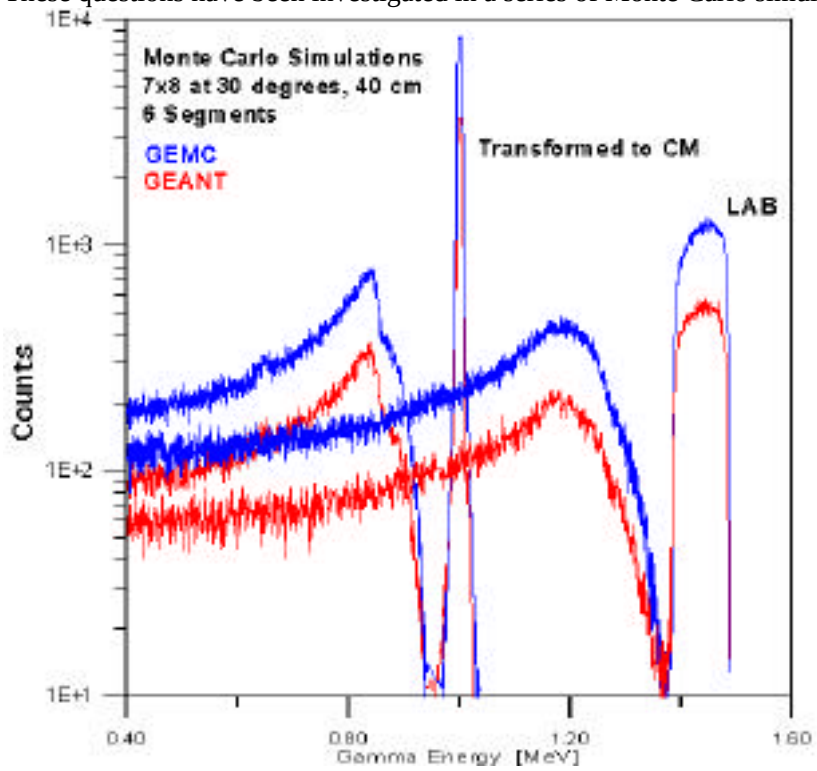

Figure 8: Response of 7 cm (dia.) x 8 cm crystal to lateral incidence of a 1 MeV gamma ray emitted at 100 MeV/u at 40 cm distance and 30^0 relative to the beam axis. The upper (broad) peaks and their associated continuum distributions are the laboratory response and the narrow peaks the result of the retroconversion to the CM system. The upper curve are calculated with GEMC (980,000 incident gammas) and the lower with GEANT (430,000 incident gammas).

3. Monte Carlo Simulations of Germanium Detector Response

We have developed a simulation program GEMC written in Fortran. It tracks the cascade generated by a gamma ray entering the crystal by simulating a sequence of events with probability distributions based on the differential cross sections associated with each of the four main interactions. These are photoelectric absorption, elastic (Rayleigh) scattering, Compton scattering, and the production of positron-electron pairs with subsequent annihilation of the positron. The calculation follows each new gamma ray produced in the last three processes until all have been either absorbed or have exited the crystal. The calculated interaction points and interaction energies are translated into the simulated response for a given configuration of the detector. The routine does not in its present version include escape of recoil electrons and positrons through the detector surface, the escape of characteristic x-rays and the formation and possible escape of bremsstrahlung quanta. (Although bremsstrahlung is produced in many events, most of it is of low energy and is immediately reabsorbed.) The calculations shown in the following include only the effects of the segmentation perpendicular to the crystal axis. The left/right identification is without importance here since we do not include the direction of the nuclear recoil in our simulation. Inclusion of forward/backward localization would have improved the detector performance at short distances when the number of segments is large.

We have tested the performance of GEMC against CERN's GEANT program [3], which has been designed for the simulation of the response of large detector systems in particle physics. The two routines turn out to give very similar results for a 1 MeV gamma ray emitted from a moving source, see Fig. 8. The photopeak-to-total ratios calculated for a 1 MeV gamma ray emitted from a stationary source are also close: 36.2% for GEMC and 33.8% for GEANT. The calculations also answer the frequently encountered question whether lateral incidence of the gamma rays is a less efficient use of the germanium than axial incidence.

The answer is that for low energy gamma rays our 7x8 cm detector presents a larger area seen from the side and is about 10% more efficient. At higher energies the two arrangements are essentially equivalent.

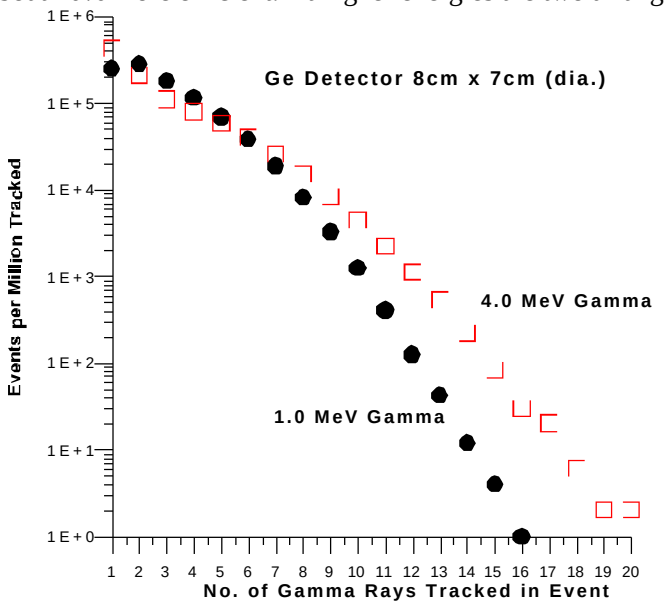

Figure: 9: Distribution of the number of gamma rays tracked per 980,000 incident primary gammas of energy 1 or 4 MeV. Events with multiplicity one are those in which the incident gamma was absorbed in a photoelectric event or, much more frequently, passed the crystal without interacting.

The complexity of the individual events registered in a single detector is shown in Fig. 9, which shows that five or even ten individual hits are not a rare occurrence. The response in the segmented detector is considerably simpler due to summing of hits in one segment. Thus we found that for a detector with 1.3 cm wide segments along the axis only 4% of all events will have more than two segments active .

The problem in referring an observed event back to the corresponding center-of-mass energy is then to identify the hit that corresponds to the first impact. We have experimented with several strategies including more complex ones such as investigating the sign of the asymmetry of the signature. This analysis has not been brought to a termination and will necessarily have to be resumed to study the effect of the full segmentation combining lateral slices with quadrants. At the present stage the simplest strategy is also the best, namely to assume that the segment with the highest energy deposited also is the one that has the primary impact. Only for energies of 0.2-0.5 MeV is there a modest advantage in using instead the weighted average of the position of impact.

The precision can be improved by noting that the gamma rays do not enter as a parallel beam and that the point of impact is the average position of the front surface augmented by the average penetration depth for a gamma ray of the corresponding energy.

In all studies of strategies for and precision of the event localization it is important not to work with the complete sample of simulated events but only with the sub-set that deposited the full gamma-ray energy. This is crucial because the multiplicities and event patterns are different for the two classes and because we have no interest in optimizing the localization of the predominant events in which energy escapes from the detector. In fact, this might blur the object of the study. There is no "correct" reconstruction of the events in which only a part of the energy was deposited in the detector, since the loss, unknown to us, actually took place in the laboratory system. Examples of this are given in Fig. 10, below.

As an example of the performance of the planned segmentation, we show in Fig. 10 the calculated response for a 2 MeV gamma ray in a detector placed so that it leaves a cone of 12^0 open around the beam axis and for three assumed distances. While the photopeak, although badly smeared, is still visible at 20 and

---

Note that the simulations, so far, have not included the subdivision of each disc into four quadrants. We intend to look into this at some later stage.

40 cm, the spectrum at 20 cm no longer has any resolved structure. The reconstruction leads to resolved peaks in all three cases, as can be seen more clearly in the enlarged version (Fig. 11) with a resolution that agrees well with the thin-target calculations in Fig. 4. (The slightly narrower lines in the latter calculation can be traced back to small differences in the basic assumptions.)

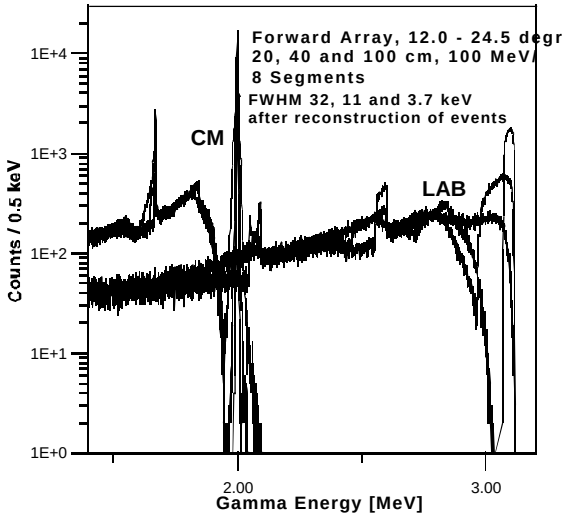

Figure 10: Response of 7 cm (dia.) x 8 cm crystal to lateral incidence of a 2 MeV gamma ray emitted at 100 MeV/u at distances 20, 40 and 100 cm with the detector placed in the forward direction, i.e. leaving an iner cone of 12^0 free. For the distance of 40 cm the angular coverage is thus from 12^0 to 24.5^0. The three curves ending above 3 MeV represent the laboratory response and the narrow peaks at 2 MeV the result of the retroconversion to the CM system. All curves are are based on a simulation with 980,000 incident gammas.

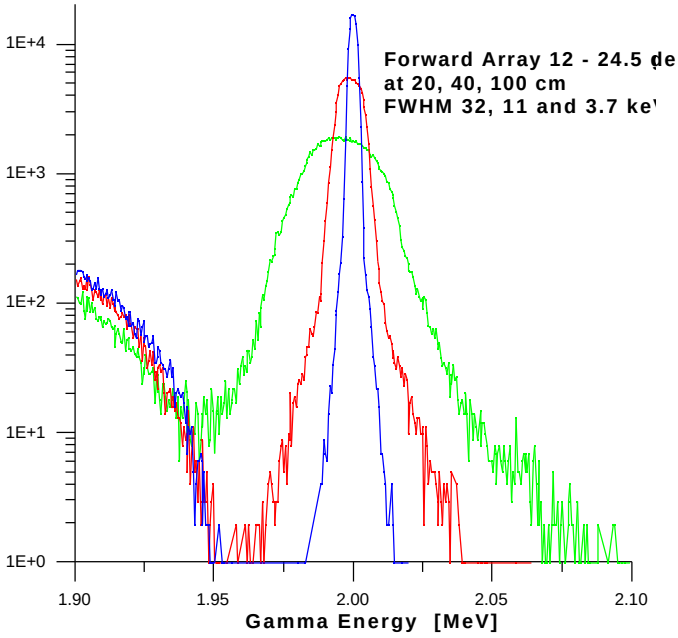

Figure 11: Expanded view of the reconstructed peaks of Fig. 10. The resolution (FWHM) is 21, 11 and 3.7 keV in the three cases as compared with an intrinsic resolution of 2.3 keV.

Fig. 10 illustrates that the back-conversion process only renders the full-energy events in a faithful way. The pair escape peaks, for example, appear 320 keV below the full energy peak, and the gap between the Compton plateau and the full energy peak is likewise smaller than it would be if observed with a stationary source.

As a second example Fig. 12 shows a 4.0 MeV gamma detected at the "magic" angle of 64.6^0 and at a distance of 40 cm. (100 cm would be required at this angle to match the resolution in the forward direction.) The resolution is now only 1.3%.

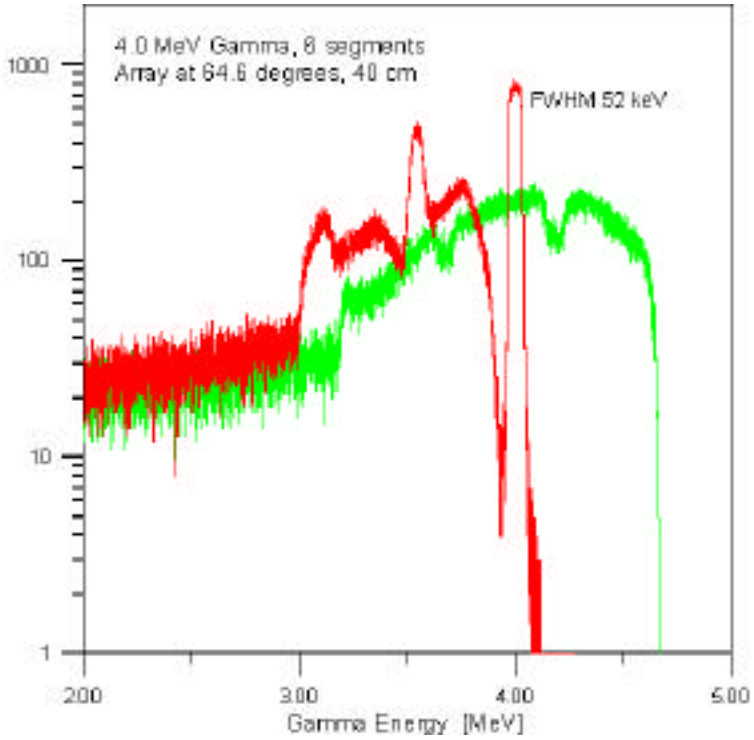

Figure 12: Response of 7 cm (dia.) x 8 cm crystal to lateral incidence of a 4 MeV gamma ray emitted at 100 MeV/u at a distance of 40 cm with the detector placed at 64.6^0. The curve ending at 4.7 MeV represents the laboratory response and the peak at 2 MeV the result of the retroconversion. The calculation is based on a simulation with 980,000 incident gammas.

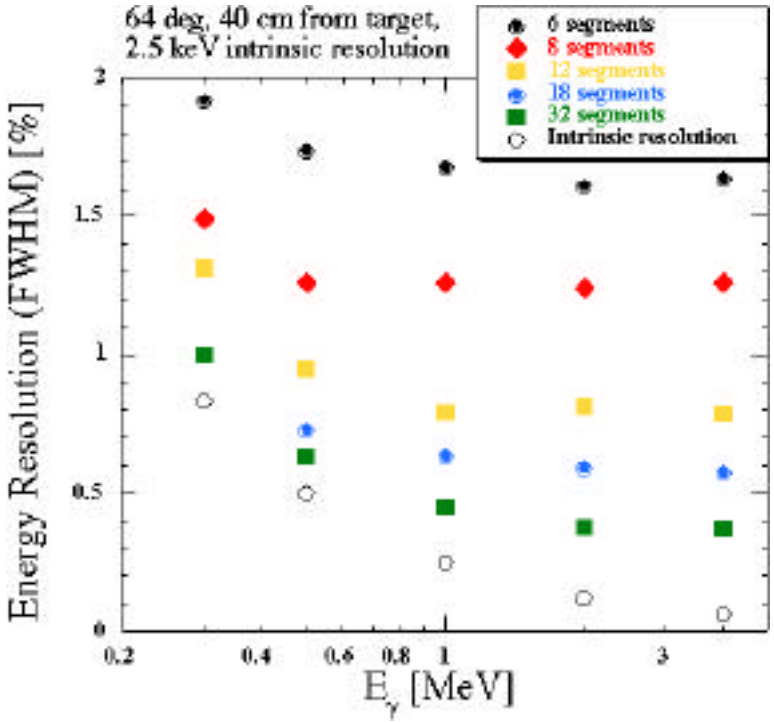

Figure 13: The energy resolution is here shown as a function of the gamma-ray energy for different numbers of segments. Since the response functions have distinctly non-Gaussian shapes (see Fig. 13) the line widths have been read manually, which accounts for some statistical scatter in the points.

3. Concluding Remarks

We have used the Monte Carlo routine GEMC to test the effect of decreasing the height of the disc-shaped segments. These have been carried out for an angle of 64.6[a], where the Doppler effects are most detrimental (see Fig. 3). The finest segmentation assumed, 0.25 cm, is at a limit where other effects neglected in our simulations must begin to play a role. Figure 13 shows the resolution as a function of the CM energy of the incident gamma ray. The improvement is present at all energies but is most pronounced above 1 MeV. The cost of the electronics increases almost linearly with the number of segments. We believe that the subdivision into quadrants is essential to preserve some (but far from equal) spatial resolving power in the left/right and forward/backward directions. If the height is subdivided into 8 segments this provides a respectable resolution of about 0.5% for the forward array (see Figs. 10 and 11), and leaves us with 33 pulse height preamplifiers and outputs (with one serving the spectroscopy channel connected to the central contact). We feel that this is an acceptable degree of complexity at the present stage.

In summary, we have chosen a conservative design based essentially on existing technology. We expect it to function as foreseen with a minimum of technical development work. At the same time we hope that current research on spatial interpolation via pulse-shape discrimination will lead to a breakthrough that will allow us an upgrade of the electronics of the array at a later stage.

Note added in prooft. An array of 18 detectors based on the design described here ws ordered in April 1998. Testing is expected to begin in the fall of 1998.

Acknowledgement. We are indebted to a number of colleagues who generously took of their precious time to discuss with us and to visit the NSCL to give us their views on the possibilities and problems in our kind of germanium-counter spectroscopy. These include Jürgen Eberth, Jürgen Gerl, Robert Janssens, I-Yang Lee, Dirk Schwalm, and especially David Radford, who first suggested a design based on a stack of planar detectors with side entry to us. We thank them all for their help.

References

[1] C.W. Beausang and J. Simpson, “Large arrays of escape suppressed spectrometers for nuclear structure experiments”, J. Phys. **G 22**, 527 (1996).

[2] T. Kröll, I. Peter, T.W. Elze, J. Gerl, T. Happ, M. Kaspar, H. Schaffner, S. Schremmer, R. Schubert, K. vetter, and H.J. Wollersleben, “Analysis of simulated and measured pulse shapes of closed-ended HPGe detectors”, Nucl. Instr. Meth. **A 371**, 489 (1996).

[3] GEANT, “CERN Program Library Long Writeup WP103” CERN, Geneva 1993.

[4] A. Bohr and B.R. Mottelson, *Nuclear Structure* (Benjamin), 1969).